Available online at www.sciencedirect.com
ScienceDirect
Ceramics International 35 (2009) 247–251
CERAMICS INTERNATIONAL
www.elsevier.com/locate/ceramint

Phase transformation and gas–solid reaction of Al_2O_3 during high-energy ball milling in N_2 atmosphere

Pengliang Li *, Shengqi Xi, Jingen Zhou

State Key Laboratory for Mechanical Behavior of Materials, School of Materials Science and Engineering, Xi'an Jiaotong University, 710049 Xi'an, People's Republic of China

Received 19 July 2007; received in revised form 3 September 2007; accepted 5 October 2007
Available online 25 December 2007

Abstract

Al_2O_3 powders were milled in N_2 atmosphere using an attritor ball mill. The phase transformation and gas–solid reaction of Al_2O_3 during high-energy ball milling in N_2 atmosphere were investigated. It is found that the γ-Al_2O_3 transform to α-Al_2O_3 as milling time increases. Milled for 20 h in N_2 atmosphere, Al_2O_3 becomes partially amorphous and the gas–solid reaction between Al_2O_3 and N_2 takes place. A new phase with cubic aluminum nitride (AlN) structure forms during milling which is different from normal hexagonal AlN produced by carbon thermal reduction processing. As milling energy increases, the amount of this new phase with cubic AlN structure increases. The amount of this new phase is as high as 72% when Al_2O_3 is milled in N_2 atmosphere at 650 rpm for 40 h.

Keywords: Cubic AlN; High-energy ball milling; Phase transformation; Gas–solid reaction

1. Introduction

Aluminum nitride (AlN) is an important ceramic material because of its excellent properties. It demonstrated high thermal conductivity (theoretical thermal conductivity is 320 W/m K) low dielectric constant (about 8.8), thermal expansion coefficient matching silicon (293–773 K, $4.8 \times 10^{-6}\,K^{-1}$) and good electrical insulation. It is thus expected to replace the others ceramic such as SiC, BeO and Al_2O_3, which are currently used as substrate materials because of their thermal properties [1]. There are many researches on the AlN sintering process [1–5], but the most critical factor in the manufacture of advanced ceramic materials is the synthesis of the starting powder. Though there are some new methods to produce ultra-fine AlN [1,6–8], the main process mostly used in industry is the carbothermal reduction. Using this method, the alumina should be heated over 1600 °C to react with carbon and nitrogen for relatively long times to form AlN. So, the cost of AlN is expensive. To decrease the cost of AlN synthesis, the reaction temperature and time of this carbothermal reduction should be decreased. One promising way is to enhance the activity of Al_2O_3 used in this method. Usually, the grain size of raw material Al_2O_3 is in range of 5–100 μm and its activity is low.

Ball milling is an effective method for synthesizing active solids. The fine effect of ball milling has been studied widely. But there are few researches on the chemical active effect of mechanical milling [9,10]. Recently, the high-energy ball milling, i.e. the mechanical alloying which was first developed by Benjamin to produce ODS Ni-base superalloys, has been used as a special technology to synthesize new materials such as amorphous phase, nanocrystalline materials [11,12], and others. Although it is widely researched all over the word, most researches focus onto the systems in which the alloying or the phase transformation and/or the chemical reaction could occur during high-energy ball milling. There were a few researches on the activity of high-energy ball milling [13–15]. But the main attentions of these researches were put on the active effect on the sintering of ball-milled powders. As a new technology, the active process during the high-energy ball milling is fundamental for synthesizing material. The active process is also very important for us to understand the mechanism of mechanical active synthesizing new materials by high-energy ball milling. So, it is very necessary to study the active process of high-energy ball milling.

* Corresponding author.
E-mail address: lipl@mailst.xjtu.edu.cn (P. Li).

0272-8842/$34.00 © 2008 Published by Elsevier Ltd and Techna Group S.r.l.
doi:10.1016/j.ceramint.2007.10.030

During high-energy ball milling, not only the powders were fined but the complex structures such as micro-strain and amorphous phase, etc. were also formed in the powders. In this paper, Al_2O_3 powders were milled in N_2 atmosphere using an attritor ball mill. The phase transformation and gas–solid reaction of Al_2O_3 during high-energy ball milling in N_2 atmosphere were investigated.

2. Experiment details

The raw materials used in this experiment are commercial Al_2O_3 powders. The characteristics of these powders are shown in Table 1. The powders were milled using an attritor ball mill in pure nitrogen atmosphere. Hardened chromium steel balls were used as grinding medium. The canister of the mill was cooled using circulation of water during milling. The speed of the drive shaft is 450/650 rpm and the ball to powder weight ratio is 20:1. After predetermined milling time, the milled powders were removed from the vial and their structure was analyzed using X-ray diffractometer (XRD) and transmission electron microscope (TEM).

To prevent contamination by Fe during ball milling, before formal experiment, Al_2O_3 powders were milled for 30 h using this attritor and these powders were discarded, so that a thin adherent coating of Al_2O_3 were formed on the internal surface of the container and also on the surface of grinding medium and the impellers.

The morphology of milled powder was analyzed using a JEM-200cx TEM and the selected area electron diffraction (SAED) of milled powder was also completed using this TEM.

The X-ray patterns of the milled powder were obtained via a D/max-B diffractometer using Cu Kα radiation and a graphite secondary monochromater. The generator settings were 40 KV and 100 mA. The diffraction data were collected over 2θ range of 15–110° with a step width of 0.004 and a counting time of 4 s per step.

3. Results and discussion

3.1. Phase evolution of Al_2O_3 powders milling for short times

It is well known that, besides α-Al_2O_3, there are still about 11 types of crystal structures for Al_2O_3, such as β-, γ-, δ-, ζ-, ξ-, θ-, η-, κ-, χ-, λ- and ρ-Al_2O_3, etc. α-Al_2O_3 is the final and steady phase at 1300 °C, all other phases could be considered as transition phases during the calcination stages of $Al(OH)_3$. There are three important crystal structures for Al_2O_3, which are θ-Al_2O_3, γ-Al_2O_3 and α-Al_2O_3. Their reaction activities are different as shown in Table 2. Fig. 1 is the XRD pattern of original commercial Al_2O_3 powders and the powders milled at 450 rpm for different milling times. It indicated that the original Al_2O_3 powders were mainly composed of γ-Al_2O_3 and α-Al_2O_3. There were a spot of $Al(OH)_3$ in these powders which remained during calcination. All of diffraction peaks of α-Al_2O_3 were narrow and those of γ-Al_2O_3 were broad. This indicated the crystallite size of α-Al_2O_3 was large and that of γ-Al_2O_3 was small. This was consistent with the result of Tsuge's research [16]. He reports that different phases of Al_2O_3 have different crystallite sizes. As the crystallite size of γ-Al_2O_3 is smaller than 100 nm, the specific surface area of γ-Al_2O_3 is very large and it has high reaction activity. This is in favor of the carbon thermal reduction processing. So, it was an aim to remain as much more γ-Al_2O_3 as possible after ball milling.

It could be found in Fig. 1 that the transformation of γ-Al_2O_3 to α-Al_2O_3 took place. When milling time more than 2 h, the intensities of all peaks of γ-Al_2O_3 decreased as milling time increased. The half-width of all peaks, not only that of γ-Al_2O_3 but also α-Al_2O_3, increased as milling prolonged. This indicated that the crystallite size of Al_2O_3 powders was fined during ball milling. As shown in Fig. 2, after milling for 1 h, the amount of γ-Al_2O_3 increased

Table 1
Characteristics of commercial Al_2O_3 powder

Material	Al_2O_3 powder
Granularity (μm)	75
Impurity (wt.%)	
Fe	0.005
Sulfate	0.03
Chloride	0.01
Pb	0.005

Table 2
Crystal structure and activation of various Al_2O_3 [16]

Phase	Crystal structure	Lattice	Mean crystallite size (μm)	Oxygen content after carbothermal reduction at 1500 °C/wt.%
θ-Al_2O_3	Monoclinic	C^2/m	0.51	26.4
α-Al_2O_3	Rhombohedral	R3C	1.0	24.7
γ-Al_2O_3	Cubic	Fd3m	0.005	1.53

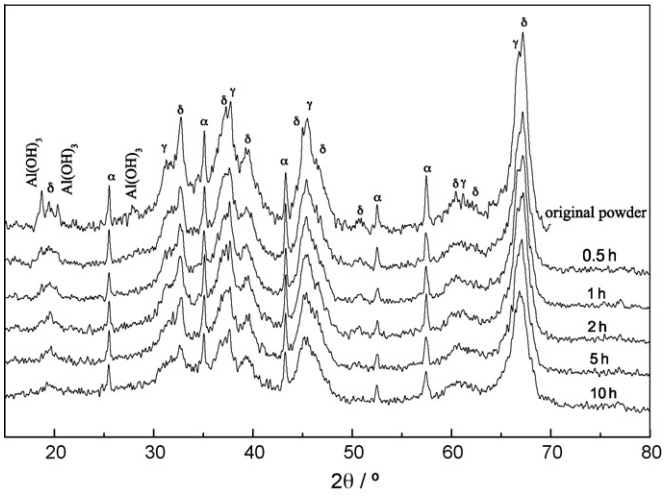

Fig. 1. XRD patterns of original Al_2O_3 powder and powders milled for different times.

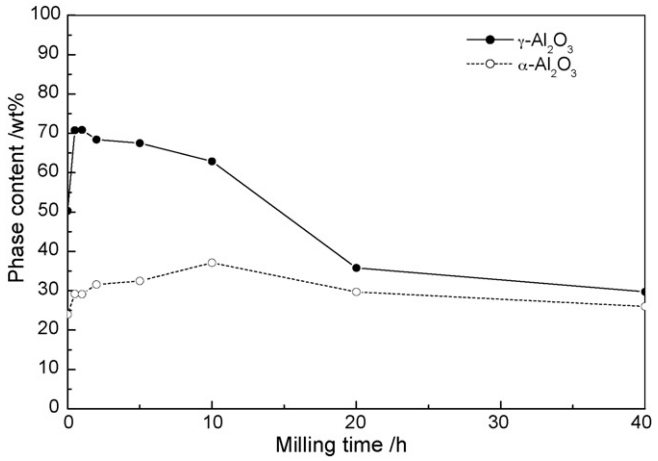

Fig. 2. Variation of the amount of different phases with various milling time.

obviously and the amount of α-Al_2O_3 increased slightly. This was due to the decomposition of $Al(OH)_3$ remained in the original Al_2O_3 powders during ball milling. After then, as milling time increased the amount of decreased obviously and correspondingly the amount of α-Al_2O_3 increased. Due to mechanical active the γ-Al_2O_3 transformed to the α-Al_2O_3. When milling time more than 10 h, a new phase with cubic AlN structure was formed. This would be discussed later.

3.2. The gas–solid reaction of Al_2O_3 with N_2 during ball milling

Fig. 3 is the XRD pattern of Al_2O_3 powder milled at 450 rpm for 20 h. It is different from the Fig. 1 obviously. There were two important phenomena presented when milling time lasts for more than 10 h. One is that the Al_2O_3 was partially amorphous. The background of the XRD pattern milled for 20 h was increased obviously compared to that of which milled for less than 10 h, especially when 2θ was between 15° and 40°, it was almost to form a broad hump. This is due to the amorphous Al_2O_3. Another important new phenomenon is the appearance of a new phase with cubic AlN structure formed in

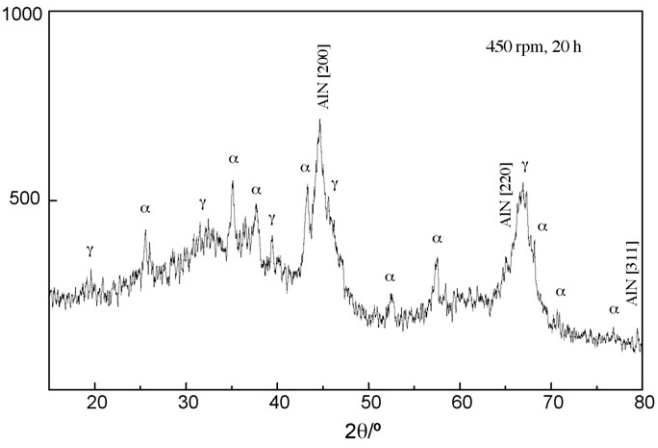

Fig. 3. XRD pattern of Al_2O_3 powder milled at 450 rpm for 20 h.

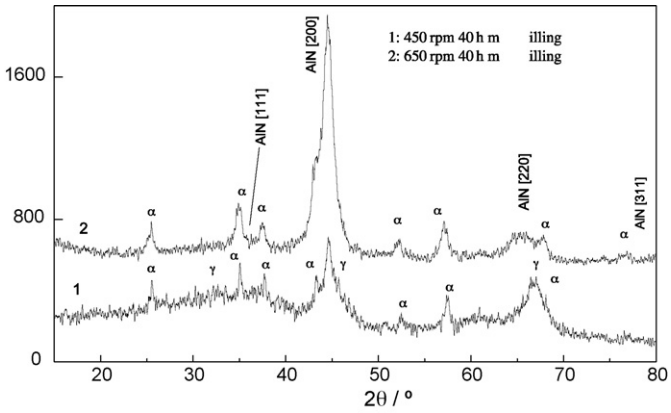

Fig. 4. XRD patterns of Al_2O_3 powder milled at 450 and 650 rpm for 20 h.

these milled powder. During ball milling, the Al_2O_3 was fined and the content of crystalline defects of Al_2O_3 increased. All these were favor for the adsorption of N_2 on the fined powders. Milled with enough energy, the bonding of Al–O could be ruptured and the N atom could react with Al, so that the new phase with cubic AlN structure could be formed during ball milling.

It could be expected that there would be an increasing content of this new phase (with cubic AlN structure) in the powder milled with higher milling energy. Fig. 4 shows the results for Al_2O_3 milled for 40 h at 450 rpm and 650 rpm. Compared to Fig. 3, there is no obvious difference between the XRD patterns of powders milled for 20 h and 40 h at the same speed (450 rpm, which means the same milling energy). After prolonged milling times, the amount of this new phase did not increase obviously when milled at the same milling energy. The remaining Al_2O_3 could not react with N_2 further at this milling energy. To promote the gas–solid reaction, the milling energy should be increased. As shown in Fig. 4, this was proved by the XRD pattern of powders milled at 650 rpm for 40 h. The amount of this new phase in these powders reached 72%, which is higher than that in the powder milled at 450 rpm for 40 h. This new phase formed was AlN with cubic structure. It could be identified in the XRD pattern. The XRD patterns of Al_2O_3

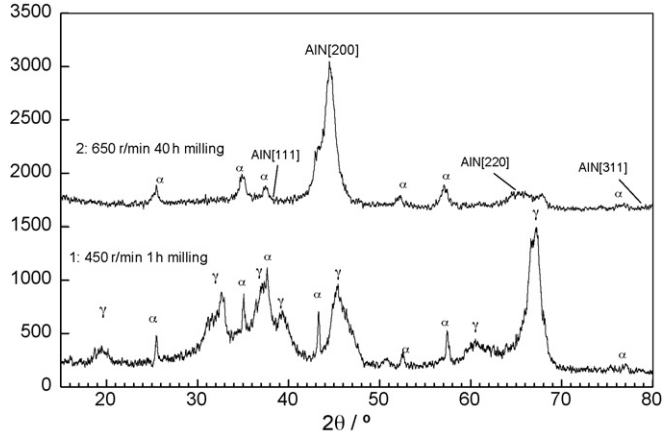

Fig. 5. XRD patterns of Al_2O_3 powders milled at 450 rpm for 1 h and milled at 650 rpm for 40 h.

Table 3
Peak positions of powders milled at different condition contrasted with the standard XRD card

Peak positions of powder milled at 450 rpm for 1 h	γ-Al_2O_3 (XRD card no. 29-0063)	Peak positions of powder milled at 650 rpm for 40 h	Cubic AlN (XRD card no. 46-1200)
$2\theta/d$ (according to the descending intensity of diffraction)			
67.260/1.3908	1.40 [440]	44.620/2.0291	2.0226 [200]
45.300/2.0002	1.98 [400]	65.204/1.4297	1.4300 [220]
37.660/2.3865	2.39 [311]	38.460/2.3387	2.3349 [111]
32.740/2.7331	2.80 [220]	None	0.9045 [420]
39.320/2.2895	2.28 [222]	None	1.1678 [222]
19.460/4.5577	4.53 [111]	78.310/1.2200	1.2195 [311]
60.620/1.5263	1.53 [511]		

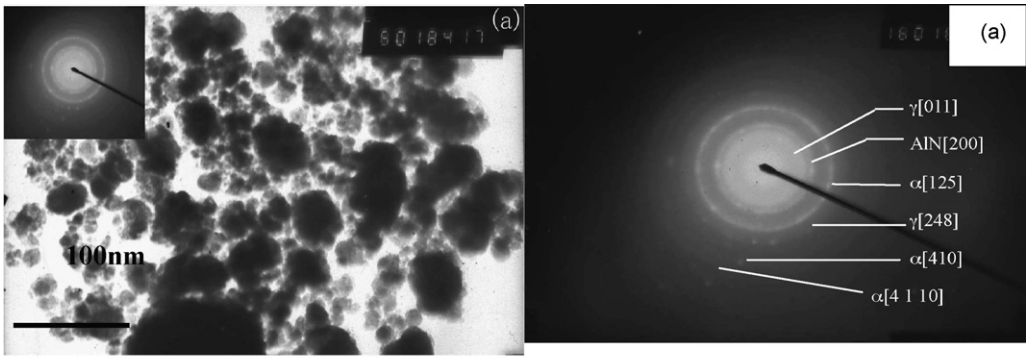

(a) 450 rpm, 20h

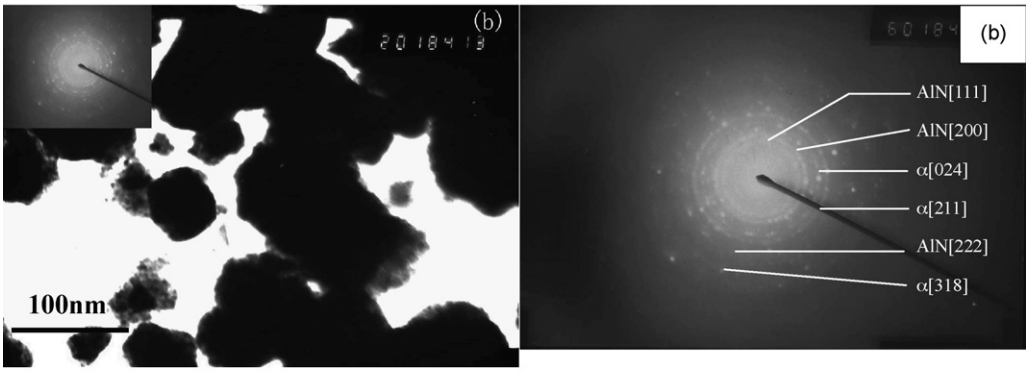

(b) 650 rpm, 40h

Fig. 6. TEM image and SEAD of Al_2O_3 powders after ball milling.

powder milled at 450 rpm for 1 h and at 650 rpm for 40 h are contrastively shown in Fig. 5 and the peak positions of γ-Al_2O_3 and cubic AlN are given in Table 3. The new phase formed in these powders is different from AlN synthesized by carbon thermal reduction, the crystalline structure of which is hexagonal. The exact reason for this phenomenon should be studied further more.

Fig. 6(a) shows the image and selected area electron diffraction of powders milled at 450 rpm for 20 h. The powder's size was about 30–50 nm. Selected area electron diffraction of powders showed that they were composed of a nanocrystalline new phase with cubic AlN structure and nanocrystalline Al_2O_3 and amorphous, which is consistent with the result of XRD analysis. When milled at high speed and for longer times, the amorphous Al_2O_3 were recrystallized due to the energy import during ball milling, as shown in Fig. 6(b).

4. Conclusions

Al_2O_3 powders were milled in N_2 atmosphere using an attritor ball mill, and the phase transformation and gas–solid reaction of Al_2O_3 during high-energy ball milling in N_2 atmosphere were investigated. The main conclusions were:

(1) γ-Al_2O_3 transforms to α-Al_2O_3 as milling time increase. This does not favor the decrease of the activation energy of the carbon thermal reduction, which is an industrial processing to produce AlN ceramics.

(2) After milling for 20 h in N_2 atmosphere, Al_2O_3 was partially amorphous and the gas–solid reaction between Al_2O_3 and N_2 took place. A new phase with cubic AlN structure formed during milling, which is different from AlN produced by carbon thermal reduction, the crystalline structure of AlN synthesized by carbon thermal reduction processing being hexagonal.
(3) As milling energy increases, the amount of cubic AlN increases. The amount of this new phase is as high as 72% when milling is operated in N_2 atmosphere at 650 rpm for 40 h.

Acknowledgements

The authors would like to acknowledge the financial support of specialized research fund for the Doctoral Program of Higher Education (No. 20040698053). This research is also supported by the Key Project of Chinese Ministry of Education (No. 105159) and by the Program for New Century Excellent Talents in University (No. NCET-05-0839).

References

[1] G. Selvaduray, L. Sheet, Mater. Sci. Technol. 9 (1993) 463.
[2] R.R. Lee, Development of high thermal conductivity aluminum nitride ceramics, J. Am. Ceram. Soc. 9 (1991) 2242–2249.
[3] T. Barrett Jackson, A.V. virkar, K.L. More, R.B. Dinwiddie Jr., R.A. Cutler, High thermal conductivity aluminum nitride ceramics: the effect of thermodynamic kinetic and microstructural factors, J. Am. Ceram. Soc. 6 (1997) 1421–1435.
[4] Z.Y. Fu, J.F. Liu, H. Wang, D.H. He, Q.J. Zhang, Spark plasma sintering of aluminum nitride transparent ceramic, Mater. Sci. Technol. 20 (2004) 1097–1099.
[5] I.-L. Tangen, Y. Yu, T. Grande, et al., Phase relations and microstructure development of aluminum nitride–aluminum nitride polytypoid composites in the aluminum nitride–alumina–yittria system, J. Am. Ceram. Soc. 9 (2004) 1734–1740.
[6] F.J.M. Haussonne, Mater. Manuf. Process. 10 (1995) 717.
[7] L. Hongdong, H. Yang, G. Zou, S. Yu, Ultrafine AlN and Al–AlN powders: preparation by DC plasma and thermal treatment, Adv. Mater. 2 (1997) 156–159.
[8] L.-W. Yin, Y. Bando, Y.-C. Zhu, et al., Single-crystalline AlN nanotubes with carbon-layer coatings on the outer and inner surfaces via a multi-walled-carbon-nanotube-template-induced route, Adv. Mater. 2 (2005) 213–217.
[9] V.V. Boldrev, S.V. Povlov, E.L. Goldberg, Interrelation between fine grinding and mechanical activation, Inter. J. Miner. Process. 44–45 (1996) 181–185.
[10] M. Yasuoka, K. Okada, T. Hayashi, et al., Property changes of mechanically treated alumina powders by annealing, Ceram. Int. 18 (1992) 131–137.
[11] B.S. Murty, S. Ranganathan, Novel materials synthesis by mechanical alloying/milling, Int. Mater. Rev. 43 (1998) 101–141.
[12] C. Suryanarayana, Mechanical alloying and milling, Prog. Mater. Sci. 46 (2001) 1–184.
[13] Y. Yoshizawa, F. Saito, Low temperature sintering of alumina with the aid of abrasive powder in wet grinding, J. Soc. Powder Technol. Jpn. 11 (1996) 842–847.
[14] G.R. Karagedov, N.Z. Lyakhov, Effect of mechanical activation on the sintering of α-alumina, Inorg. Mater. (Russ.) 7 (1997) 688–691.
[15] A. Osami, Contamination and sinterability of planetary milled α-alumina, Kona Hirakata Jpn. 13 (1995) 159–166.
[16] A. Tsuge, Raw material effect on AlN synthesis from Al_2O_3 carbothermal reduction, J. Mater. Sci. 25 (1990) 2359–2361.